DOI 10.31489/2020Ph3/13-21

UDC 544.526.2

T.M. Serikov*

Karagandy University of the name of academician E.A. Buketov, Kazakhstan
*(*E-mail: serikov-timur@mail.ru)*

The effect of electric transport properties of titanium dioxide nanostructures on their photocatalytic activity

Annotation. Films formed by nanoparticles, nanorods and nanotubes of titanium dioxide with a thickness of 3.9, 4.0 and 4.1 μm, respectively, with an area of 2 cm^2 were obtained by various methods. Nanostructures were characterized by X-ray phase analysis, scanning electron microscopy (SEM), BET (Brunauer–Emmett–Teller), BJH (Barrett–Joyner–Halenda). The electric transport properties of the films were studied by impedance spectroscopy. The photocatalytic activity of the samples was evaluated by the photocurrent and degradation of the methylene blue dye under xenon lamp illumination. The concentration of hydrogen released per unit time was determined by gas chromatography in a standard quartz cuvette using a platinum electrode. The study of texture characteristics showed that the obtained isotherms belong to type IV isotherms with a hysteresis loop, reflecting the process of capillary condensation in mesopores. The diffraction peaks for the films of nanoparticles and nanotubes of titanium dioxide are identical and correspond to the tetragonal phase of anatase, for films of nanorods to the tetragonal phase of rutile. When studying the electric transport properties of films, it was found that films of titanium dioxide nanoparticles have a higher resistance associated with unformed bonds between nanoparticles. Despite the low specific surface area, titanium dioxide nanorods showed higher photocatalytic activity than nanotubes and nanoparticles. The results are confirmed by measurements of photocurrent, dye decomposition and the splitting of water molecules into hydrogen gas and oxygen.

Keywords: nanoparticles, nanotubes, nanorods, titanium dioxide, BET, electric transport properties, photocatalytic activity, hydrogen

Introduction

Development and research to create effective photocatalysts for the degradation of organic compounds and toxic substances in drinking water, the splitting of water molecules into hydrogen and oxygen are the promising direction in «green energy». Semiconductors, often used as photocatalysts, have the ability to generate reactive oxygen species (ROS) O_2^-, $_1O_2$, H_2O_2 и OH. Over the past decade, nanostructures based on titanium dioxide (TiO_2) have been the most effective photocatalysts, due to their chemical stability, low cost, fairly high oxidizing capacity, optical properties and features of electronic transport [1].

It is known that the photocatalytic activity of nanomaterials is influenced by many factors, the most significant of which are the specific surface area, particle size, crystal phase, morphology, and electronic transport. Heterogeneous catalysis between catalysts and reagents occurs mainly on the surface or at the interface, so the efficiency depends partly on the specific surface area of the materials. A large specific surface area will provide a large active contact area, allowing the adsorbed water molecules and hydroxyl to react faster, and are also a place for fixing organic molecules for photodegradation [2–4]. The specific surface area increases dramatically with decreasing crystal size, so small spherical nanoparticles (NP) have a large surface area, making them the most common type of TiO_2-based photocatalyst.. On the other hand, one-dimensional (1D) TiO_2 nanostructures, such as nanotubes (NT), nanorods (NR), have unique properties and advantages for photocatalytic reactions due to their 1D geometry [5,6]. Structures with direct electron paths significantly increase the electric transport properties of films by excluding grain boundaries that occur when using films made of TiO_2 nanoparticles. NP, NR, NT TiO_2 can be in 3 main crystal phases: brucite, anatase and rutile. It is believed that the best photocatalytic activity is observed for anatase due to the lower recombination rate and high adsorption capacity [7, 8]. Although there are other opinions, for example, it has been experimentally proved that a mixture of the crystal phases of anatase and rutile shows better photocatalytic activity than separately [9, 10]. Therefore, what kind of photocatalyst will work better is still not known: a high specific surface area of NP TiO_2 or improved electron transport of NR and NT TiO_2.

In this work, three types of nanostructures were used: NP, NR and NT TiO_2, which differ in geometric characteristics, but have relatively the same thickness and area of the films. The most common, cheap and

simple methods of nanostructure synthesis were used, such as hydrothermal synthesis for NR [11] and electrochemical anodizing for NT [12, 13]. The characteristic difference between NT and TiO_2 nanorods is that the former have an open internal channel, which should significantly increase their specific surface area.

Experimental

The synthesis of films formed by the NP TiO_2

The film of NP TiO_2 was prepared as follows: 50 mg of TiO_2 colloidal titanium dioxide (Sigma Aldrich company Degussa P25) was ground in a porcelain mortar with the addition of 2 ml of deionized water and 0.2 ml of acetone and mixed for 24 hours using a magnetic stirrer to form a homogeneous paste. The finished paste was applied to the surface of pre-cleaned photo substrates (Sigma Aldrich, 8 Ohms/cm^2) by the «doctor–blading» method and dried at a temperature of 100 ºC for 30 minutes. The film thickness was controlled using tape applied to the edges of the substrate. Then the samples were calcined at a temperature of 500 ºC for 2 hours.

The synthesis of films formed by the NR TiO_2

Nanostructured films based on HR TiO_2 were obtained by hydrothermal synthesis as follows: a solution containing 15 ml of deionized water (H_2O), 15 ml of hydrochloric acid (HCl) (36.5–38.0 %, Sigma–Aldrich) and 0.25 ml of titanium butoxide $C_{16}H_{36}O_4Ti$ (titanium butoxide, 97 %, Sigma–Aldrich) was prepared in a 50 ml stainless steel vessel. Then, pre-cleaned glasses with a conducting layer of ITO (Sigma-Aldrich, 8 Ohms/cm^2) were placed in the same vessel with the conducting side down. The stainless steel vessel is closed and placed in a convective oven at a temperature of 180 ºC for 24 hours. The resulting samples were washed with deionized water and dried at room temperature. Then the samples were calcined at a temperature of 500 ºC for 2 hours.

The synthesis of films formed by the NT TiO_2

The films were obtained by 2-stage electrochemical anodizing of pre-chemically polished, purified titanium foil (VT1–0, 99.7 %, Russia) at a temperature of 5–7 ºC. The thickness of the foil was 60 microns. As the base of the electrolyte, $C_2H_6O_2$ was used, with a content of 0.3 wt.% NH_4F and 2 wt% H_2O. The cathode was platinum foil. The distance between the cathode and the anode was 3 cm. The anodizing voltage is 40 V. During the anodizing process, the solution was intensively mixed using a magnetic stirrer. During the first stage of anodizing, a film of NT TiO_2 and hydrolysis byproducts is formed on the surface of the titanium foil within 2 hours, which were removed from the surface of the foil in an ultrasonic bath, in a solution of hydrochloric acid. The duration of the second stage of anodizing was 4 hours. The amorphous phase of TiO_2 was crystallized by heat treatment of samples in a muffle furnace at a temperature of 500 ºC within 2 hours.

X-ray phase analysis of films was studied using a rint 2000 diffractometer (model D5005). Images of the sample surface were obtained using a scanning electron microscope (SEM) MIRA 3 LMU (Tescan, Czech Republic). The textural characteristics of synthesized samples were calculated on the basis of nitrogen adsorption and desorption isotherms at a temperature of 77 K obtained at the quantachrome volumetric unit («Quantachrome Instruments», USA). The specific surface area of the samples was estimated by the Brunauer–Emmett–Taylor method (BET). To study the photocatalytic activity of films, the values of the photoinduced current and photodegradation of the methylene blue dye were measured. The photocurrent of nanostructures with an illuminated area of 1 cm^2 was measured at a constant potential of 0 V using a potentiostat (ELINS R-20XV, Russia) in a standard three-electrode cell. TiO_2 nanostructures were used as the working electrode. The opposite electrode was a platinum foil, and an AgCl electrode was used as the reference electrode. Measurements were made in an electrolyte of 0.1 M NaOH in a specially made photoelectrochemical cell with a quartz window. When registering the photocurrent, titanium dioxide films were irradiated with a 45 mW/cm^2 xenon lamp. The photoactivity of the films was evaluated in the reaction of photodegradation of an aqueous MB solution. Plates with a size of 1×2 cm were vertically lowered into a quartz reactor containing 50 ml of a MB solution with an initial concentration of 10^{-5} mol/l and kept for 20 hours to exclude errors in measuring the optical density of the dye associated with the adsorption of molecules into its pores. The solution is continuously mixed using a magnetic stirrer. The system was irradiated with a 45 mW/cm^2 xenon lamp.

The electrotransport properties of films were studied using the method of impedance spectroscopy. Measurements of the impedance spectra were performed on the biologic (Science Instruments) impedance meter. The amplitude of the applied signal was up to 25 mV, and the frequency range from 1 MHz to 100 MHz.

Results and discussion

Diffraction peaks shown in figure 1(101), (004), (200), (105), (211), (204), (116), (220) and (215) for NP and NT TiO_2 films are identical and correspond to the tetragonal phase of anatase (JCPDS, no. 84–1286, $a = b = 0.1949$ nm and $c = 0.1980$ nm).

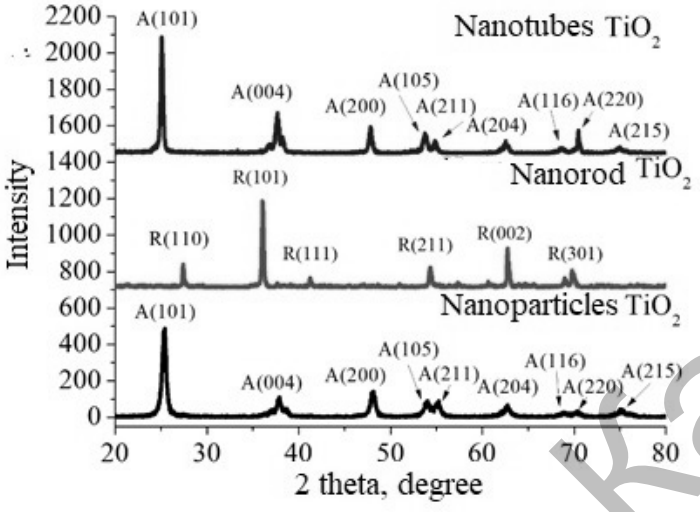

Figure 1. Radiographs of nanostructured films TiO_2

All diffraction peaks presented for NR films are in good agreement with the tetragonal phase of rutile TiO_2 (JCPDS, no. 21–1276, $a = b = 0.4517$ nm and $c = 0.2940$ nm). The presence of sharp peaks for NR indicates that the films have good crystallinity. The diffraction peaks (002) and (101) were significantly amplified, indicating that the deposited film is highly oriented relative to the substrate surface.

Figure 2 shows the results of a study of the surface morphology of TiO_2 nanostructured films.

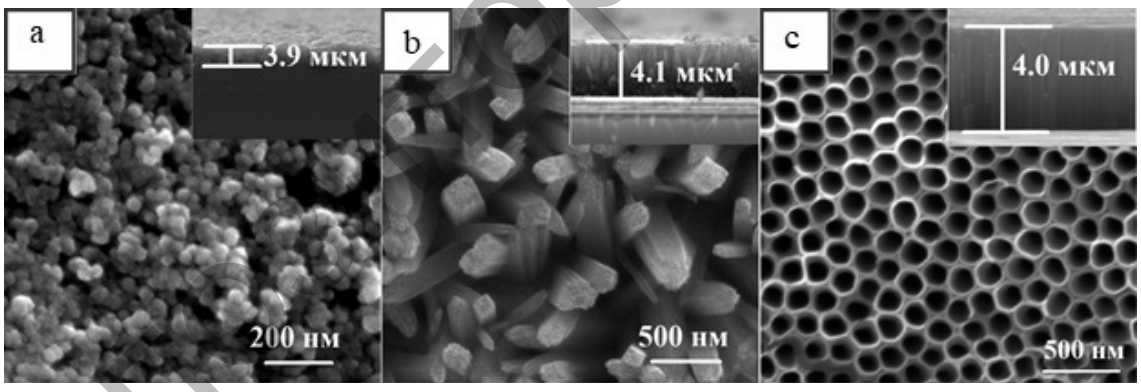

Figure 2. SEM images of TiO_2 nanostructured films

Figure 2*a* shows that the presented NP TiO_2 film has a clearly defined granular structure. The average particle diameter is 25 nm. Figure 2*b* shows that as a result of hydrothermal synthesis, nanorods made of titanium dioxide are formed on the surface of the FTO glass, located perpendicular to the substrate plane. The average diameter of the nanorods is 100–120 nm, and the length is 4.1 microns. Figure 2*c* shows that as a result of careful control of external conditions, films were obtained from tightly packed cylindrical geometrically anisotropic titanium dioxide fragments located perpendicular to the foil plane. The porous structure of the film and the size of individual channels, which are about 90 nm, are clearly visible. It is shown that the surface of TiO_2 films is low-defect, and they themselves have a clearly marked channel along their entire length. The thickness of all titanium dioxide nanostructures was selected so that their thickness was about ~4 microns. The thickness of the film from NP was controlled using tape (thickness of 1 layer ~2 microns), if necessary, the number of layers applied was repeated. The film thickness of NR TiO_2 was controlled by the

temperature and duration of hydrothermal synthesis, and NT TiO_2 by the time (4 hours) and the voltage (40 V) of anodizing. The active area of all samples was 1 cm^2.

The textural characteristics of TiO_2 nanostructures were calculated based on nitrogen adsorption and desorption isotherms at a temperature of 77 K. To obtain the adsorption-desorption curve, a powder from NP TiO_2 was used, and for NT and NR, the films were mechanically separated from the base. The isotherms are shown in Figure 3*a*.

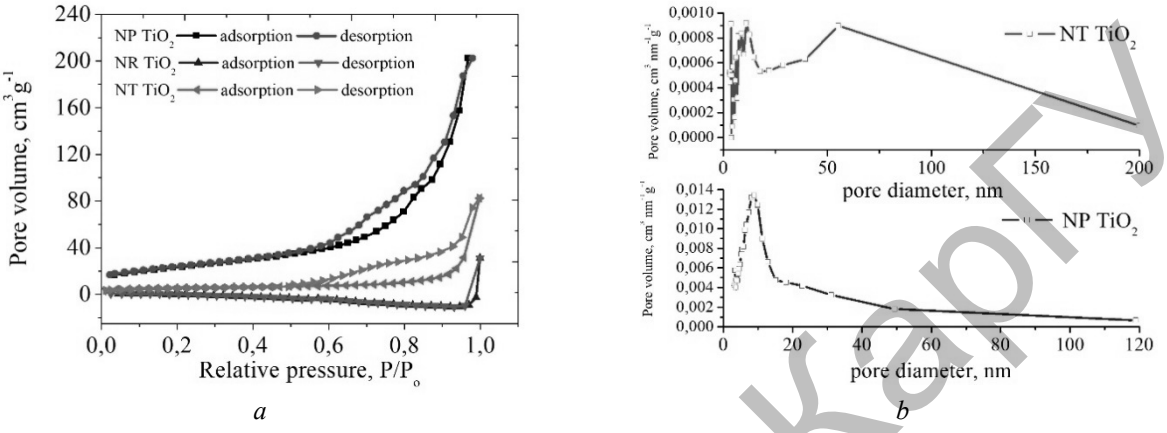

a *b*

Figure 3. Adsorption-desorption isotherms and pore size distribution of TiO_2 nanostructures

From the presented data, it can be seen that the nitrogen adsorption-desorption isotherms for all samples have the same appearance, except for the volume of adsorbed nitrogen. At low relative pressures (P/P_0 less than 0.1), an increase in nitrogen adsorption is observed on the isotherms, which indicates the presence of micropores. With an increase in the relative partial pressure for samples of NP and NT TiO_2, the volume of adsorbed nitrogen increases, and an increase in the relative pressure range from 0.45 to 0.99 indicates the presence of a mesoporous (2–50 nm) structure. For NR TiO_2, the isotherm is characterized by a decrease in the amount of adsorbate with an increase in P/P_0, as well as negative values of this value. With repeated measurements and an increase in the weight of the hitch does not lead to changes in the isotherm. Experiments were carried out when the weight of the hitch was comparable to the weight of the hitch NT. Further increase in the weight of the hitch for samples from the NR was not possible, since its separation from the surface of the substrate was difficult, the output was minimal. This may indicate a low surface of the test sample (<1 m^2/g). In accordance with the IUPAC nomenclature, the obtained isotherms belong to type IV isotherms with a hysteresis loop, reflecting the process of capillary condensation in mesopores. The volume of mesopores was calculated using the Barrett–Joyner–Halenda method and the pore size distribution was obtained (Fig. 3*b*) for NP and NT. For NR films, calculations were not performed using this method. From the pore distribution curve for the NP film, one peak can be distinguished in the region of the pore diameter of 10 nm. For films made of NT TiO_2, two peaks can be identified in the region of the pore diameter of 10 and 55 nm. Pores with a diameter of less than 10 nm are probably located on the inner or outer surface of the walls of TiO_2 nanotubes. It should be noted that the samples also show the presence of macropores. The value of the surface area for films made of NR TiO_2 was estimated by the number of adsorbed molecules of the methylene blue dye ($S_{molecule}$=130 $Å^2$) on its surface. The results of the research are presented in Table 1.

Table 1

Textural characteristics of TiO_2 nanostructures

Sample	Surface area	Pore volume, cm^3/g
NP TiO_2	73.218 m^2/g	0.306 cm^3/g
NR TiO_2	62 cm^2/ cm^2	-
NT TiO_2	19.437 m^2/g	0.122 cm^3/g

From the presented data, it can be seen that the specific surface area of NP TiO_2 is 4 times higher than NT TiO_2.

Electric transport properties of nanostructured films were studied by measuring the electrical impedance. Figure 4 shows the impedance hodographs in Nyquist coordinates for NP, NR, and NT TiO_2.

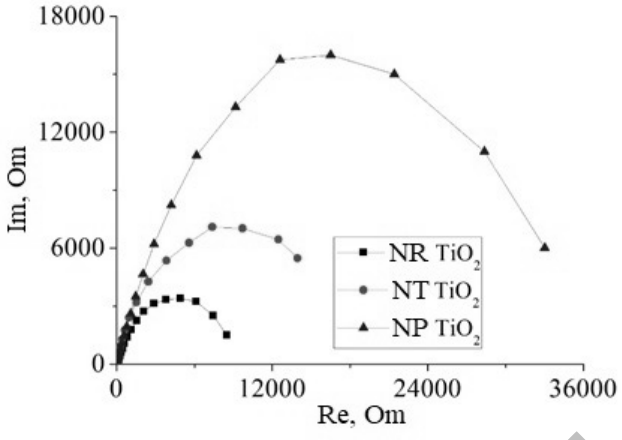

Figure 4. Impedance spectrum of titanium dioxide nanostructures

The values of the chain elements obtained in the framework of the model used are shown in Table 2. One of the important parameters that can be determined from the measurement of the solar cell impedance is the lifetime of charge carriers in a semiconductor film (τ). Since the impedance measurements were made when the film was illuminated, it can be concluded that τ characterizes the lifetime of photoelectrons. The calculations were performed using the methods described in [14, 15].

The effective electron diffusion coefficient D_{eff}, the effective recombination rate k_{eff}, the effective electron lifetime T_{eff}, the resistance to electron transport in R_w titanium dioxide films, and the charge transfer resistance R_k associated with electron recombination were calculated from the central arc of the impedance spectra. The results are presented in Table 2.

Table 2

Electric transport parameters of solar cells based on TiO_2 nanostructures

Sample	D_{eff}, cm^2/c^{-1}	k_{eff}, c^{-1}	τ_{eff}, c	R_k. Ohm	R_w, Ohm	Con, Ohm·cm c^{-1}	L, mkm
NP TiO_2	$6.7 \cdot 10^{-3}$	16	0.062	33015	11.9	206	3.9
NT TiO_2	$2.3 \cdot 10^{-3}$	12	0.083	13952	12.0	68	4.1
NR TiO_2	$3.6 \cdot 10^{-4}$	9.6	0.104	8480	36.0	32.5	4.0

The recombination rate (k_{eff}) is directly proportional to the electron density in the trap state and the recombination rate constant c of the traps. In NP films, its value is 16, and for NR it is 9.6, which may indicate that the density of electrons in the trap states is less in NR. The lifetime of the T_{eff} electrons in the NP is lower than in films made of NT and NR. This may be due to the rapid recombination of electrons and holes. The resistance to electronic transport in TiO_2 (R_w) for NP films is higher than in NR and NT.

Based on this we can draw the following conclusion: High resistance in the films of NP is connected with the unformed relations between the nanoparticles. Unformed bonds lead to an increase in surface defects through which recombination occurs. The use of nanostructures with one-dimensional electron transport reduces the resistance and speed of recombination processes. Despite the low specific surface area of NR and NT than NP, they can be promising materials for photocatalysis. The photocatalytic properties of films are shown in the Figure 5 below.

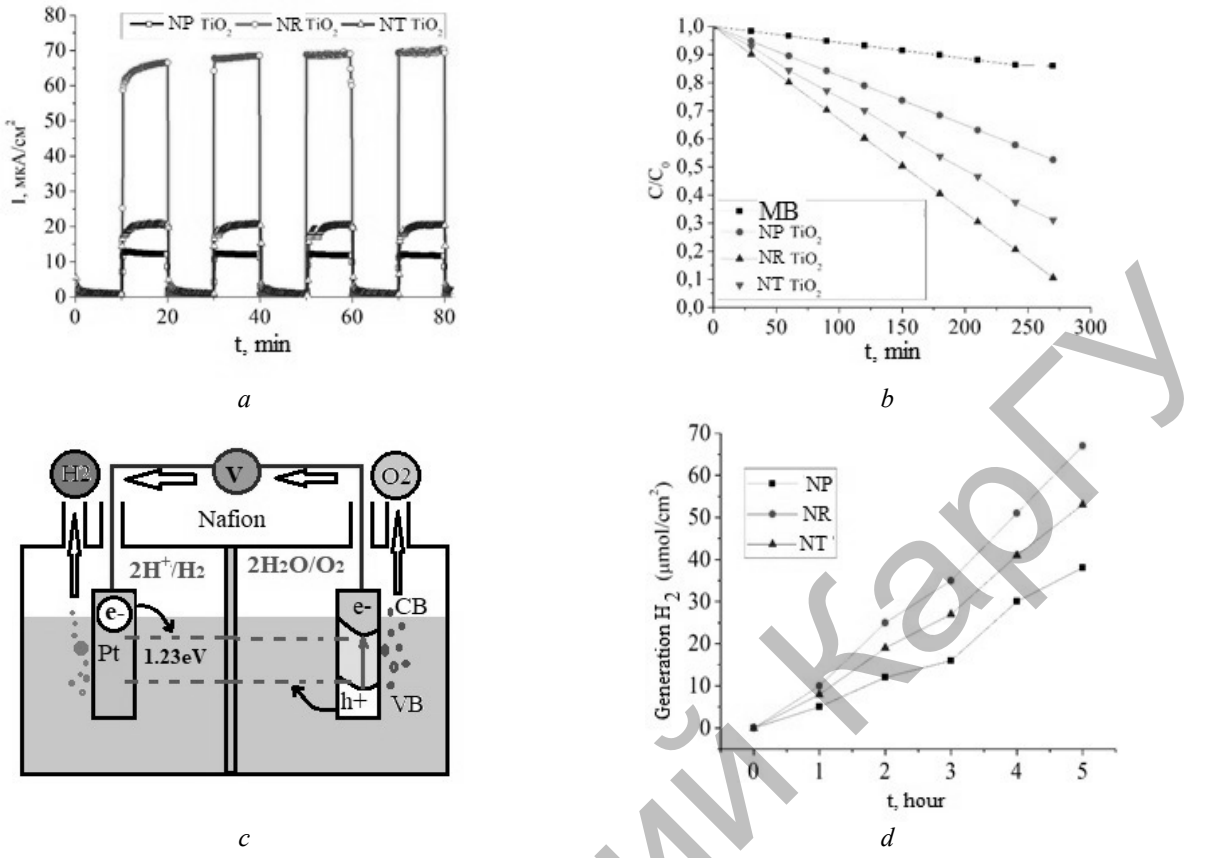

Figure 5. Photocatalytic properties of titanium dioxide nanostructures

Figure 5*a* shows the photo-feedback of titanium dioxide nanostructures when irradiated by an electromagnetic wave and its absence. All samples show fairly good stability. It should be noted that with an identical area and comparably the same thickness of films, the photocurrent for NR is 3 times higher than for NT, and 5 times higher than for NP titanium dioxide. At the same time, the value of the active surface area (Table 1) is much lower for NR than for NP and NT. Given the above, we can conclude that the formation of photocurrent is associated with one-dimensional electron transport along the surface of the nanorods. NT titanium dioxide has a one-dimensional electron transport and a high specific surface area. The low value of the photocurrent can be associated with a number of circumstances: when forming NT, titanium foil is used, which has foreign impurities, such as Al, Zn, F, etc., which is simply impossible to exclude; during electrochemical anodizing, hydrolysis products, TiF_6, can be formed on the surface of nanotubes; during heat treatment of NT samples, an additional oxide layer or barrier may occur due to partial peeling of the oxide layer between the NT and the titanium foil. The low value of the photocurrent for NP can be associated with unformed bonds between nanoparticles, which leads to rapid recombination of electrons and holes, as evidenced by the results of the study by impedance spectroscopy. The photocatalytic activity of nanostructures in the MB dye degradation reaction was studied (see Fig. 5*b*). When irradiated with a xenon lamp MB ye, its concentration changed slightly. When irradiated for 4.5 hours in the presence of titanium dioxide films, its concentration decreased linearly, which indicates its degradation. The results obtained show that the best photocatalytic activity is the film from NR. Degradation to 95 % is achieved in 270 min., and for NT and NP this time is much higher. It should be noted that this work was done solely to compare the photocatalytic activity of titanium dioxide nanostructures with each other. Since the obtained results on the degradation of the dye do not correspond to the values given in similar scientific papers published in journals. First of all, this is due to the radiation source used. Usually, xenon lamps with a power of 100mW/cm^2 or 300 W are used in the works. In this work, 45 mw/cm^2.

Figure 5*c* shows a cell in which photocatalytic water splitting occurs. The cell material is quartz (Minihua Store). The opposite electrode is platinum. Separation of solutions was performed using a Nafion filter. Titanium dioxide nanostructures were used as the working electrode. Both sides of the cell were prepurged with a stream of argon gas. Then, when irradiated, the sample was sampled and identified using an

Agilent gas chromatograph. Figure 5*d* shows that when using films from NR, hydrogen generation is higher than for films from NT and NP.

Conclusions

Films were synthesized from NP, NR and NT of titanium dioxide with a thickness of 3.9, 4.0 and 4.1 microns, with an area of 2 cm^2. The textural characteristics of films are studied. The obtained isotherms belong to type IV isotherms with a hysteresis loop, reflecting the process of capillary condensation in mesopores. The volume of mesopores was calculated using the Barrett–Joyner–Halenda method and the pore size distribution was obtained. For NP films, the specific surface area was 73.218 m^2/g, and for NR and NT, 62 cm^2/cm^2 and 19.437 m^2/g, respectively. The diffraction peaks for NP and NT TiO_2 films are identical and correspond to the tetragonal phase of anatase, for NR films, with the tetragonal phase of rutile. Electric transport properties of nanostructured films were studied by measuring the electrical impedance. From the central arc of the impedance spectra were computed effective diffusion coefficient D_{eff} of electrons, the effective recombination rate k_{eff}, the effective lifetime τ_{eff} of the electron, the resistance of electron transport in films of titanium dioxide R_w, resistance of charge transfer R_k associated with the recombination of an electron. High resistance in the films of NP is connected with the unformed bonds between nanoparticles. Unformed relations lead to the increase of surface defects, which occur through recombination. The use of nanostructures with one-dimensional electron transport reduces the resistance and speed of recombination processes. Despite the low specific surface area of NR and NT than NP, they can be promising materials for photocatalysis. The photocurrent for RS is 3 times higher than for NT, and 5 times higher than for NP of titanium dioxide. The photocatalytic activity of nanostructures in the MB dye degradation reaction was investigated. When the dye was irradiated for 4.5 hours in the presence of titanium dioxide films, its concentration decreased linearly, which indicated its degradation. The results obtained show that the best photocatalytic activity is the film from NR. Degradation to 95 % is achieved in 270 min., and for NT and NP this time is much higher. When splitting water molecules into hydrogen gas and oxygen, it was found that when using films from NR, its release occurs significantly more than in NP and NT.

References

1 Rosales M. The influence of the morphology of 1D TiO_2 nanostructures on photogeneration of reactive oxygen species and enhanced photocatalytic activity / M. Rosales, T. Zoltan, C. Yadarola // Journal of Molecular Liquids. — 2019. — Vol. 281. — P. 59–69. DOI:10.1016/j.molliq.2019.02.070

2 Tian G. Preparation and characterization of stable biphase TiO_2 photocatalyst with high crystallinity, large surface area, and enhanced photoactivity / G. Tian, L. Fu, B. Jing, K. Pan // J. Phys. Chem. C. — 2008. — Vol. 112. — P. 3083. DOI: 10.1021/jp710283p

3 Chen C.H. Effect of phase composition, morphology, and specific surface area on the photocatalytic activity of TiO_2 nanomaterials / C.H. Chen, Q.W. Liu, S.M. Gao, K. Li, H. Xu, Z.Z. Lou, B.B. Huang, Y. Dai // RSC Adv. — 2014. — Vol. 105. — P. 12098. DOI:10.1039/C4RA05509H

4 Joo B. Control of the nanoscale crystallinity in mesoporous TiO_2 shells for enhanced photocatalytic activity / B. Joo, Q. Zhang, M. Dahl, I. Lee, J. Goebl, F. Zaera, Y. Yin // Energy & Environmental Science. — 2012. — Vol. 5. — P. 6321–6327. DOI: 10.1039/c1ee02533c

5 Yuan Z.-Y. Titanium oxide nanotubes, nanofibers and nanowires / Z.-Y. Yuan, B.-L. Su //Colloids Surf. A Physicochem. Eng. Asp. — 2004. — Vol. 241. — P. 173–183. DOI: 10.1016/j.colsurfa.2004.04.030.

6 Benjwal P. 1-D and 2-D morphology of metal cation co-doped (Zn, Mn) TiO_2 and investigation of their photocatalytic activity / P. Benjwal, B. De, K.K. Kar // Appl. Surf. Sci. — 2018. — Vol. 427. — P. 262–272. DOI: 10.1016/j.apsusc.2017.08.226.

7 Liu H. Preparation and properties of nanocrystalline alpha-Fe_2O_3-sensitized TiO_2 nanosheets as a visible light photocatalyst / H. Liu, L. Gao // J. Am. Ceram. Soc. — 2006. — Vol. 89. — P. 370–373. DOI: 10.1111/j.1551–2916.2005.00686.x.

8 Kongsong P. Effect of nitrogen doping on the photocatalytic activity and hydrophobic property of rutile TiO_2 nanorods array / P. Kongsong, A. Taleb, M. Masae, A. Jeenarong, P. Hansud, S. Khumruean // Surf Interface Anal. — 2018. — Vol. 44. — P. 1–7. DOI: 10.1002/sia.6518.

9 Su R. Density functional theory study of mixed-phase TiO_2: heterostructures and electronic properties / R. Su, R. Bechstein, L. So, R.T. Vang, M. Sillassen, B. Esbjornsson, A. Palmqvist, F. Besenbacher // J. Phys. Chem. C. — 2011. — Vol. 115. — P. 24287. DOI: 10.1007/s00894–014–2215–7

10 Ravidhas C. Tunable morphology with selective faceted growth of visible light active TiO_2 thin films by facile hydrothermal method: structural, optical and photocatalytic properties / C. Ravidhas, B. Anitha, D. Arivukarasan // Journal of Materials Science: Materials in Electronics. — 2016. — Vol. 27. — P. 5020–5032. DOI: 10.1007/s10854–016–4389–5

11 Ibrayev N.Kh. Investigation of the structural, optical and photocatalytic properties of TiO_2 nanotubes / N.Kh. Ibrayev, T.M. Serikov, A.K. Zeinidenov // Eurasian physical technical journal. — 2017. — Vol. 14, No. 2(28). — P. 72–78.

12 Serikov T.M. Surface and sorption properties of TiO_2 nanotubes, synthesized by electrochemical anodization / T.M. Serikov, N.K. Ibrayev, Z. Smagulov // IOP Conference Series — Materials Science and Engineering. — 2016. — Vol. 110. — P. 012066. DOI: 10.1088/1757–899X/110/1/012066

13 Serikov T.M. Influence of surface properties of the titanium dioxide porous films on the characteristics of solar cells / T.M. Serikov, N.K. Ibrayev, N.N. Nuraje, S.V. Savilov, V.V. Lunin // Russian Chemical Bulletin. — 2017. — Vol. 66, No. 4. — P. 614–621. DOI: 10.1007/s11172–017–1781–0

14 Fabregat-Santiago F. Electrochemical impedance spectra of dye-sensitized solar cells: fundamentals and spreadsheet calculation / F. Fabregat-Santiago, J. Bisquert, G. Garcia-Belmonte // Solar Energy Materials & Solar Cells. — 2005. — Vol. 87. — P. 117. DOI: 10.1155/2014/851705

15 Adachi M. Determination of parameters of electron transport in dye-sensitized solar cells using electrochemical impedance spectroscopy / M. Adachi, M. Sakamoto, J. Jiu // Journal Physics Chemistry B. — 2006. — Vol. 110. — P. 13872. DOI: 10.1021/jp061693u

Т.М. Сериков

Титан диоксиді наноқұрылымдарының электрлік тасымалдау қасиеттерінің олардың фотокаталитикалық белсенділігіне әсері

Әртүрлі әдістерді қолдана отырып, ауданы 2 $см^2$, ал қалыңдықтары 3,9, 4,0 және 4,1 мкм болатын нанобөлшектерден, нанотүтікшелерден және наноөзекшелерден тұратын қабыршақтар синтезделді. Наноқұрылымдар рентгенді-фазалық анализ, сканерлеуші электронды микроскопия, БЭТ (Брунауэр, Эмметт және Тейлор), БДХ (Баретт–Джойнер–Халенд) әдістерінің көмегімен сипатталды. Қабыршақтардың электр тасымалдау қасиеттері импедансты спектроскопия әдісімен зерттелген. Үлгілердің фотокаталитикалық белсенділігі ксенон лампасының жарықтандыруы кезінде метилен көгілдір бояғышының деградациясы және фототоқты тіркеу арқылы бағаланды. Бірлік уақытта шығарылған сутегінің концентрациясы платина электродының, арнайы кварцтық кюветасының және газ хроматографиясының көмегімен анықталған. Беттік қасиеттерін зерттеу барысында алынған изотермалар IV типіне жатады және мезопорларда капиллярлық конденсация процесінің өтетінін көрсетеді. Титан диоксидінің нанобөлшектері мен нанотүтікшелерінің дифракциялық шыңдары бірдей және анатаздың тетрагональды фазасына, наноөзекшелердің қабыршақтары рутилдің тетрагональды фазасына сәйкес келеді. Қабыршақтардың электрлік қасиеттерін зерттеу кезінде титан диоксидінің нанобөлшектері қабыршақтарының нанобөлшектер арасында өзара түзілмеген байланыстарға байланысты жоғары электр кедергіге ие екендігі анықталды. Беттік ауданы төмен болғанына қарамастан, титан диоксиді наноөзекшелері нанотүтікшелер мен нанобөлшектерге қарағанда жоғары фотокаталитикалық белсенділік көрсетті. Алынған нәтижелер фототоқты өлшеу, бояғыштың ыдырауы және су молекулаларының сутегі газы мен оттегіне бөлінуі арқылы расталған.

Кілт сөздер: нанобөлшектер, нанотүтікшелер, наноөзекшелер, титан диоксиді, БЭТ, электр тасымалдау қасиеттері, фотокаталитикалық белсенділік, сутегі.

Т.М. Сериков

Влияние электротранспортных свойств наноструктур диоксида титана на их фотокаталитическую активность

Различными методами были получены пленки, образованные наночастицами, наностержнями и нанотрубками диоксида титана, толщиной 3,9; 4,0 и 4,1 мкм, соответственно, с площадью 2 $см^2$. Наноструктуры были охарактеризованы методом рентгенофазового анализа, сканирующим электронным микроскопом, методами БЭТ (Брунауэр, Эммет и Тейлор) и БЖХ (Баретт–Джойнер–Халенд). Электротранспортные свойства пленок исследованы методом импедансной спектроскопии. Фотокаталитическую активность образцов оценивали по фототоку и деградации красителя метиленового голубого при освещениях светом ксеноновой лампы. Концентрацию выделяемого водорода в единицу времени определяли методом газовой хроматографии в стандартной кварцевой кювете с использованием платинового электрода. Исследования текстурных характеристик показали, что полученные изотермы относятся к изотермам типа IV с петлей гистерезиса, отражая процесс капиллярной конденсации в мезопорах. Дифракционные пики для пленок наночастиц и нанотрубок диоксида титана идентичны и соответствуют тетрагональной фазе анатаза, для пленок из наностержней — тетрагональной фазе рутила. При исследовании электротранспортных свойств пленок было установлено, что пленки из наночастиц диоксида титана обладают более высоким сопротивлением, связанным с неформованными связями между наночастицами. Несмотря на низкую удельную поверхность, наностержни диоксида титана демонстрировали более высокую фотокаталитическую активность, чем нанотрубки и наночастицы. Полученные результаты подтверждаются измерениями фототока, разложением красителя и расщеплением молекул воды на газообразный водород и кислород.

Ключевые слова: наночастицы, нанотрубки, наностержни, диоксид титана, БЭТ, электротранспортные свойства, фотокаталитическая активность, водород.

References

1 Rosales, M., Zoltan, T., & Yadarola, C. (2019). The influence of the morphology of 1D TiO_2 nanostructures on photogeneration of reactive oxygen species and enhanced photocatalytic activity. *Journal of Molecular Liquids*, *281*, 59–69.

2 Tian, G., Fu, L., Jing, B., & Pan, K. (2008). Preparation and characterization of stable biphase TiO_2 photocatalyst with high crystallinity, large surface area, and enhanced photoactivity. *J. Phys. Chem. C, 112*, 3083.

3 Chen, C.H.,. Liu, W., Gao, S.M., Li, K., Xu, H., Lou, Z.Z., Huang, B.B., & Dai, Y. (2014). Effect of phase composition, morphology, and specific surface area on the photocatalytic activity of TiO_2 nanomaterials. *RSC Adv, 105,* 12098.

4 Joo, B., Zhang, Q., Dahl, M., Lee I., Goebl, J., Zaera, F., & Yin, Y. (2012). Control of the nanoscale crystallinity in mesoporous TiO_2 shells for enhanced photocatalytic activity. *Energy & Environmental Science*, *5*, 6321–6327.

5 Yuan, Z.-Y., & Su, B.-L. (2004). Titanium oxide nanotubes, nanofibers and nanowires. *Colloids Surf. A Physicochem. Eng. Asp*, *241*, 173–183.

6 Benjwal, P., De, B., & Kar, K.K. (2018). 1-D and 2-D morphology of metal cation co-doped (Zn, Mn) TiO_2 and investigation of their photocatalytic activity. *Appl. Surf. Sci., 427,* 262–272.

7 Liu, H., & Gao, L. (2006). Preparation and properties of nanocrystalline alpha-Fe_2O_3-sensitized TiO_2 nanosheets as a visible light photocatalyst. *J. Am. Ceram. Soc., 89,* 370–373.

8 Kongsong, P., Taleb, A., Masae, M., Jeenarong, A., Hansud, P., Khumruean, S. (2018). Effect of nitrogen doping on the photocatalytic activity and hydrophobic property of rutile TiO_2 nanorods array. *Surf Interface Anal*., *44*, 1–7.

9 Su, R., Bechstein, R., So, L., Vang, R.T., Sillassen, M., Esbjornsson, B., Palmqvist, A., & Besenbacher, F. (2011). Density functional theory study of mixed-phase TiO_2: heterostructures and electronic properties. *J. Phys. Chem. C., 115*, 24287.

10 Ravidhas, C., Anitha, B., & Arivukarasan, D. (2016). Tunable morphology with selective faceted growth of visible light active TiO_2 thin films by facile hydrothermal method: structural, optical and photocatalytic properties. *Journal of Materials Science: Materials in Electronics, 27*, 5020–5032.

11 Ibrayev, N.Kh., Serikov, T.M., & Zeinidenov, A.K. (2017). Investigation of the structural, optical and photocatalytic properties of TiO_2 nanotubes. *Eurasian physical technical journal, 14, 2(28)*, 72–78.

12 Serikov, T.M., Ibrayev, N.K., & Smagulov, Z. (2016). Surface and sorption properties of TiO_2 nanotubes, synthesized by electrochemical anodization. *IOP Conference Series — Materials Science and Engineering, 110*, 012066.

13 Serikov, T.M., Ibrayev, N.K., Nuraje, N.N., Savilov, S.V., & Lunin V.V. (2017). Influence of surface properties of the titanium dioxide porous films on the characteristics of solar cells. *Russian Chemical Bulletin, 66(4)*, 614–621.

14 Fabregat-Santiago, F., Bisquert, J., & Garcia-Belmonte, G. (2005). Electrochemical Impedance Spectra of Dye-Sensitized Solar Cells: Fundamentals and Spreadsheet Calculation. *Solar Energy Materials & Solar Cells, 87*, 117.

15 Adachi, M., Sakamoto, M., & Jiu, J. (2006). Determination of parameters of electron transport in dye-sensitized solar cells using electrochemical impedance spectroscopy. *Journal Physics Chemistry B., 110*, 13872.